

The light-fermion contribution to the exact Higgs-gluon form factor in QCD

Robert V. Harlander¹, Mario Prausa², and Johann Usovitsch³

¹*Institute for Theoretical Particle Physics and Cosmology,
 RWTH Aachen University, D-52056 Aachen, Germany*

²*Physikalisches Institut, Albert-Ludwigs-Universität,
 D-79085 Freiburg, Germany*

³*Trinity College Dublin, School of Mathematics, Dublin 2, Ireland*

Abstract

An analytical expression for the three-loop form factors for ggH and $\gamma\gamma H$ is derived for the contributions which involve massless quark loops. The result is expressed in terms of harmonic polylogarithms. It fully agrees with previously obtained kinematical expansions, and confirms a recent semi-numerical approximation which extends over the full kinematic range.

Keywords: Higgs production, hadron colliders, radiative corrections, QCD.

1 Introduction

The study of the Higgs boson is one of the most promising ways to search for physics beyond the Standard Model (SM). A necessary precondition for this to be successful is the precise understanding of the relevant SM predictions. One of the most important quantities in this respect is the cross section for Higgs production in gluon fusion. In fact, significant theoretical efforts have been made to pin down its SM value, and to estimate the associated uncertainties (see Ref. [1] for a recent review). One source of uncertainties is the fact that, up to now, QCD corrections to the Higgs cross section beyond next-to-leading order (NLO) are based on the approximation of an infinitely heavy quark mediating the

gluon-Higgs coupling. For the top-quark contribution, which by far dominates the total cross section at the Large Hadron Collider (LHC), comparison of this limit to the full result at NLO shows agreement at the sub-% level for a Higgs mass of $M_H = 125 \text{ GeV}$, providing confidence in using this approximation also at higher orders of perturbation theory [2, 3]. In fact, an explicit calculation of sub-leading terms in $1/m_t$ at next-to-next-to-leading order (NNLO), combined with the high-energy limit of the cross section, further justifies this procedure [4–7]. Nevertheless, the lack of the exact top mass dependence still requires one to associate with it an uncertainty on the total cross section of the order of 1%. It is thus a non-negligible contribution to the overall uncertainty of about 5%, which also includes uncertainties induced by parton density functions (PDFs) and α_s , for example (see Refs. [8, 9]).

A related uncertainty arises from the bottom-quark induced Higgs-gluon coupling. While suppressed by the bottom Yukawa coupling, its effect on the leading order (LO) cross section is still a reduction by about 6%. Since the numerical value of the bottom-quark mass prohibits the analogous approximation as for the top quark, QCD corrections to the bottom-quark induced ggH amplitude are known only through NLO, without significant progress since their original calculation of more than 25 years ago [3]. Serious attempts to capture the dominant logarithmic contributions of the form $\ln m_b/M_H$ to higher orders in perturbation theory have been presented only recently [10]. Thus, also for this source, the LHC Higgs Cross Section Working Group assigned an uncertainty of roughly another 1% to the total gluon fusion Higgs cross section [8].

The total cross section at NNLO requires the inclusion of three-loop virtual corrections to the ggH amplitude (the “Higgs-gluon form factor”), two-loop corrections to single-real emission, and the one-loop double-real emission contributions which occur for the first time at this order. The real-emission contributions are sufficient if one aims for Higgs boson production at non-zero transverse momenta p_\perp . In this case, top-mass effects have been addressed by several groups recently [11–14]. After estimates based on $1/m_t$ expansions of the cross section which indicated a break-down of this approximation for $p_\perp \gtrsim 150 \text{ GeV}$ [15, 16], it came as a surprise to find the K-factor of the exact calculation to be fairly independent of p_\perp [12, 13]. This provides yet another indication that also for the total cross section, the QCD corrections are well described by their heavy-top limit. Also bottom-quark mass effects have been considered for finite p_\perp [17, 18] at this order of perturbation theory.

Concerning the virtual corrections, it took about ten years before the original numerical *two-loop* result for the Higgs-gluon form factor of Ref. [3], contributing to the total cross section at NLO, was expressed in closed analytic form using harmonic polylogarithms [19–21]. The analytic result for the $\gamma\gamma H$ amplitude had been obtained one year earlier [22].

For the three-loop form factor, only approximate results are available up to now, most notably through expansions in the heavy-quark limit [23–26]. While this expansion is expected to work very well for on-shell Higgs production mediated by a top-quark loops, it will break down for the bottom-mediated contribution, or in cases where the Higgs is produced as a virtual intermediate particle, for example in off-shell or double-Higgs production. Knowledge of the general dependence of the three-loop Higgs-gluon form factor on the quark/Higgs mass ratio is thus very desirable.

Very recently, the expansions in $1/m_t$ were combined with the leading behavior of the amplitude at the top-threshold, i.e. $\hat{s} \approx 4m_t^2$ (see also Ref. [27]) in order to construct Padé approximants for the three-loop ggH amplitude which should be valid—within intrinsic Padé uncertainties—for general Higgs and quark masses [28].

In this paper, we provide an analytic result for a subset of the virtual three-loop corrections, namely those involving light (massless) quark loops in addition to the massive (top- or bottom) quark loop. Using integration-by-parts (IBP) identities, we reduce the occurring Feynman integrals to a set of master integrals, which we manage to solve in terms of harmonic polylogarithms. Comparing our result to Ref. [28], we find full agreement for this light-fermion component within the uncertainty estimate of Ref. [28]. As a byproduct of this calculation, we also obtain the three-loop $\gamma\gamma H$ form factor from which one may directly derive the exclusive photonic decay rate of the Higgs boson through NNLO.

2 Calculation

The amplitude for the processes ggH and $\gamma\gamma H$ can be parameterized with the momenta $q_{1,2}$ of the two external vector bosons as

$$\mathcal{M}_{ggH}^{ab;\mu\nu} = \delta^{ab} [(q_1^\mu q_1^\nu + q_2^\mu q_2^\nu) A_{ggH} + q_1^\mu q_2^\nu B_{ggH} + q_2^\mu q_1^\nu C_{ggH} + (q_1 \cdot q_2) g^{\mu\nu} D_{ggH}] , \quad (2.1a)$$

$$\mathcal{M}_{\gamma\gamma H}^{\mu\nu} = (q_1^\mu q_1^\nu + q_2^\mu q_2^\nu) A_{\gamma\gamma H} + q_1^\mu q_2^\nu B_{\gamma\gamma H} + q_2^\mu q_1^\nu C_{\gamma\gamma H} + (q_1 \cdot q_2) g^{\mu\nu} D_{\gamma\gamma H} , \quad (2.1b)$$

where we already implied Bose symmetry. Here and in what follows, a and b denote color indices of the adjoint representation, while μ and ν are d -dimensional Lorentz indices. Because of the trivial color structure in eq. (2.1a) which can be projected out using $(\delta_{ab}/N_A) \mathcal{M}_{ggH}^{ab;\mu\nu}$, where N_A is the number of gauge generators, we ignore the color structure in the following and focus only on the Lorentz structure of the amplitudes. For both amplitudes the Ward identity¹

$$q_{1\mu} \epsilon_{j,\nu}(q_2) \mathcal{M}^{\mu\nu} = 0 \quad (2.2)$$

¹In statements valid for both amplitudes we neglect the specification ggH or $\gamma\gamma H$ in the notation.

yields a constraint

$$D = -C. \quad (2.3)$$

In case of photons in the external state the even stronger Ward identity $q_{1\mu}\mathcal{M}_{\gamma\gamma H}^{\mu\nu} = 0$ leads in addition to a vanishing form factor $A_{\gamma\gamma H}$.

For physical quantities the only contribution stems from the form factors C . Therefore, the physical part of the amplitudes can be written as

$$\mathcal{M}_{ggH}^{ab;\mu\nu} = \delta^{ab} [q_2^\mu q_1^\nu - (q_1 \cdot q_2) g^{\mu\nu}] C_{ggH}, \quad (2.4a)$$

$$\mathcal{M}_{\gamma\gamma H}^{\mu\nu} = [q_2^\mu q_1^\nu - (q_1 \cdot q_2) g^{\mu\nu}] C_{\gamma\gamma H}. \quad (2.4b)$$

Since gluons and photons do not directly couple to the Higgs boson, the Feynman diagrams contributing to the ggH and $\gamma\gamma H$ amplitudes always involve at least one closed massive quark loop if higher orders in the electroweak coupling are neglected. In this paper, we address the calculation of the component of the form factors C which, in addition to this massive quark loop, involve a closed loop of a light quark (assumed massless here). Since the corresponding Yukawa coupling vanishes, the Higgs boson will still only couple to the diagram via the massive quark loop.

In section 2.1 we describe the toolchain used to express the contribution from light quarks to the form factors C in terms of master integrals. In section 2.2 the method for the calculation of the master integrals is explained.

2.1 Toolchain

For the calculation of the light-quark contribution to the ggH and $\gamma\gamma H$ form factors it is required to evaluate the Feynman diagrams in fig. 1. These Feynman diagrams are generated in a first step using the tool **qgraf** [29]. After the insertion of Feynman rules in R_ξ -gauge with the help of **q2e** [30, 31] the diagrams are mapped to a set of seven topologies via **exp** [30, 31].

A custom code for the computer algebra system **FORM** [32] was written in order to further process the output of **exp**. We use the projector

$$\mathcal{P}_{\mu\nu} = \frac{(q_1 \cdot q_2) g_{\mu\nu} - q_{2\mu} q_{1\nu}}{(q_1 \cdot q_2)^2 (2 - d)} \quad (2.5)$$

to project out the form factor C which already implies the validity of the Ward identity

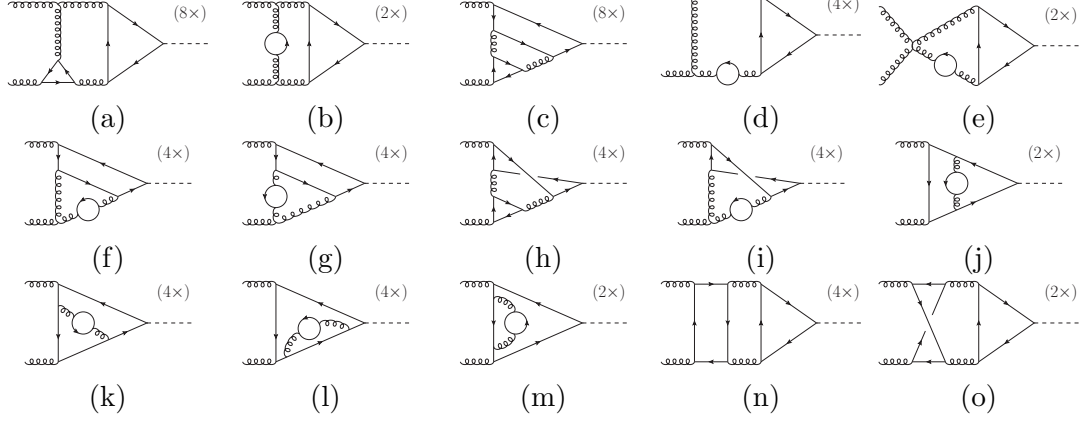


Figure 1: Feynman diagrams for ggH contributing to the light-quark contribution. Diagrams with reversed fermion flows or swapped external vector bosons are not shown but indicated by the multiplicity in the top right corner of each diagram. Only diagrams (j)–(o) contribute to the light-quark terms of $\gamma\gamma H$ with the external gluons replaced by photons.

in eq. (2.3). Moreover, we use

$$\mathcal{P}_{\mu\nu}^{(A)} = \frac{q_{1\mu}q_{1\nu}}{(q_1 \cdot q_2)^2}, \quad (2.6a)$$

$$\mathcal{P}_{\mu\nu}^{(B)} = \frac{(1-d)q_{1\nu}q_{2\mu} - q_{1\mu}q_{2\nu} + (q_1 \cdot q_2)g_{\mu\nu}}{(q_1 \cdot q_2)^2(2-d)}, \quad (2.6b)$$

$$\mathcal{P}_{\mu\nu}^{(C)} = \frac{-q_{1\nu}q_{2\mu} + (1-d)q_{1\mu}q_{2\nu} + (q_1 \cdot q_2)g_{\mu\nu}}{(q_1 \cdot q_2)^2(2-d)}, \quad (2.6c)$$

$$\mathcal{P}_{\mu\nu}^{(D)} = \frac{q_{1\nu}q_{2\mu} + q_{1\mu}q_{2\nu} - (q_1 \cdot q_2)g_{\mu\nu}}{(q_1 \cdot q_2)^2(2-d)} \quad (2.6d)$$

to project out all the form factors in eq. (2.1) in order to check our calculational setup by explicitly verifying the validity of the Ward identities, see eq. (2.3) and below. The color factor of each diagram is determined via the FORM package `color` [33].

After projecting out the form factors, the results can be expressed in terms of scalar Feynman integrals, which are subsequently reduced to 45 master integrals using integration-by-parts identities [34, 35] and the Laporta algorithm [36], implemented in the computer program `Kira`² [37, 38].

²We note that `Kira` is also able to completely reduce the full form factors C (including the n_l^0 -terms) in Feynman gauge to 403 master integrals.

After the reduction to master integrals the dependence on the gauge parameter ξ drops out and the validity of eq. (2.3) as well as $A_{\gamma H} = 0$ is confirmed.

2.2 Calculation of master integrals

A very successful technique for the evaluation of two-scale Feynman integrals is based on the method of differential equations [39–42]. The solution of the resulting coupled system of differential equations simplifies significantly if it can be written in the canonical form proposed in Ref. [43], where the right-hand side of the system is proportional to $\epsilon = (4 - d)/2$. An algorithm to compute a basis transformation to such a canonical form was presented by Lee in Ref. [44]. We utilize its implementation in the computer program **epsilon** [45] in order to evaluate the relevant master integrals.

The class of transformations Lee’s algorithm is able to find is restricted to be rational in the kinematic variable. Hence, a proper choice for the kinematic variable is inevitable to obtain a canonical form. For our purposes, an appropriate variable is

$$x = \frac{\sqrt{1 - 1/\tau} - 1}{\sqrt{1 - 1/\tau} + 1}, \quad (2.7)$$

where $\tau = M_H^2/(4m_q^2) + i0$, with the mass M_H of the Higgs boson and the mass m_q of the massive quark.

Ordering the master integrals by the number of lines in their topology yields a block-triangular structure of the system of differential equations. For most applications it is sufficient to transform only the on-diagonal blocks into the previously described canonical form. The differential equations for master integrals of a certain block $\vec{f}(x, \epsilon)$ can then be written as

$$\frac{\partial}{\partial x} \vec{f}(x, \epsilon) = \epsilon M(x) \vec{f}(x, \epsilon) + B(x, \epsilon) \vec{g}(x, \epsilon), \quad (2.8)$$

where $\vec{g}(x, \epsilon)$ consists of already solved master integrals of a lower topology, and $M(x)$ is fuchsian, i.e. it possesses only simple poles in x . For the master integrals entering the light-quark contributions, these poles lie at $x = -1, 0, 1$. The homogeneous part of (2.8) can be solved using an evolution operator $U(x, x_0; \epsilon)$ which fulfills

$$\frac{\partial}{\partial x} U(x, x_0; \epsilon) = \epsilon M(x) U(x, x_0; \epsilon) \quad ; \quad U(x_0, x_0; \epsilon) = \mathbb{1}, \quad (2.9)$$

via iterated integrations in terms of multiple polylogarithms. This evolution operator allows expressing the full solution as

$$\vec{f}(x, \epsilon) = \int_{x_0}^x dx' U(x, x'; \epsilon) B(x', \epsilon) \vec{g}(x', \epsilon) + U(x, x_0; \epsilon) \vec{f}(x_0, \epsilon), \quad (2.10)$$

where $\vec{f}(x_0, \epsilon)$ are the boundary conditions of the master integrals at $x = x_0$. In order to simplify the integral in (2.10) we chose to transform the off-diagonal blocks $B(x, \epsilon)$ of the system of differential equations into fuchsian form via `epsilon`. Doing that ensures $\vec{f}(x, \epsilon)$ to be a linear combination of multiple polylogarithms without rational function prefactors in case $\vec{g}(x, \epsilon)$ is of this form as well.

The boundary conditions $\vec{f}(x_0, \epsilon)$ are calculated as an asymptotic expansion around $x_0 = 1$, which corresponds to a limit where the quark mass m_q is large compared to the Higgs mass M_H . For this purpose, we expand the master integrals by subgraphs [46–49] as it is implemented in the computer program `exp` [30, 31].

Via the method described in this section we were able to solve not only the 45 master integrals relevant for the light-quark contributions, but in total 202 master integrals for the full amplitudes (including n_l^0 terms). The master integrals entering the light-quark contributions were cross checked against numerical results obtained by the package `FIESTA` [50].

3 Results

In this section, we define the parameterization of our results, which we have evaluated for a general gauge group with fundamental and adjoint quadratic Casimir eigenvalues C_F and C_A , and fundamental trace normalization T_F . For QCD, it is $C_F = 4/3$, $C_A = 3$, and $T_F = 1/2$. The actual analytic expressions are deferred to the appendix for the sake of readability of the main text. In this section, we restrict ourselves to a numerical presentation of the results.

3.1 Results for $C_{\gamma\gamma H}$

The form factor $C_{\gamma\gamma H}$ is presented as a perturbative series in the strong coupling constant α_s , renormalized in n_l -flavor QCD in the $\overline{\text{MS}}$ scheme:

$$C_{\gamma\gamma H} = \frac{1}{v} \frac{\alpha}{\pi} \left[C_{\gamma\gamma H}^{(0)} + \frac{\alpha_s}{\pi} C_{\gamma\gamma H}^{(1)} + \left(\frac{\alpha_s}{\pi} \right)^2 C_{\gamma\gamma H}^{(2)} + \mathcal{O}(\alpha_s^3) \right], \quad (3.1)$$

where v denotes the vacuum expectation value and α the electromagnetic coupling constant. In order to fix the notation we provide the one-loop result as

$$C_{\gamma\gamma H}^{(0)} = \frac{C_A Q_q^2}{T_F} \left[-\frac{2x}{(1-x)^2} + \frac{x(1+x)^2}{(1-x)^4} H_{0,0} \right], \quad (3.2)$$

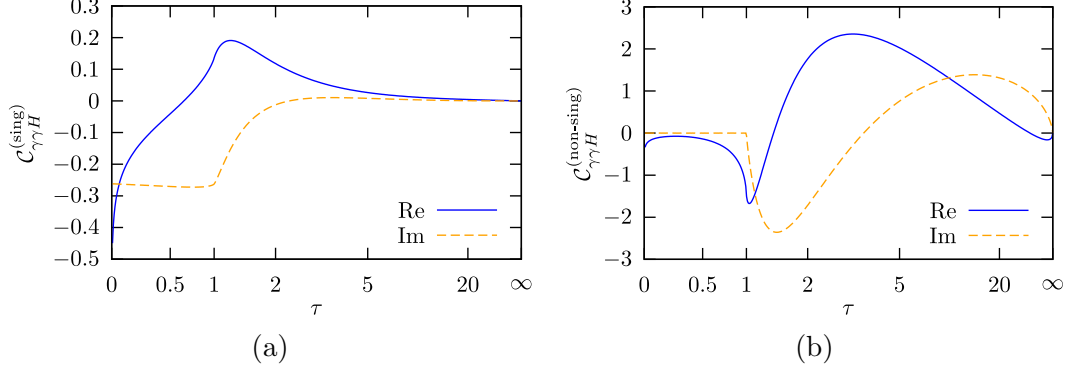


Figure 2: Singlet and non-singlet part of $C_{\gamma\gamma H}^{(2)}$ with the quark mass renormalized in the on-shell scheme and $\mu^2 = M_H^2$.

with the electric charge Q_q of the massive quark and $H_{0,0} = \ln^2(x)/2$. The three-loop result can be parameterized via

$$C_{\gamma\gamma H}^{(2)} = C_{\gamma\gamma H}^{(2,0)} + C_A C_F Q_q^2 n_l C_{\gamma\gamma H}^{(\text{non-sing})} + C_A C_F \sum_{j=1}^{n_l} Q_j^2 C_{\gamma\gamma H}^{(\text{sing})}, \quad (3.3)$$

where Q_j are the electric charges of the n_l light quarks. The term $C_{\gamma\gamma H}^{(2,0)}$ denotes the part of the amplitude without a massless quark loop, which we have not computed. The contribution stemming from a massless quark loop is split into a non-singlet part $C_{\gamma\gamma H}^{(\text{non-sing})}$ and a singlet part $C_{\gamma\gamma H}^{(\text{sing})}$. The singlet part contains the contributions from the diagrams figs. 1(n)–(o), where the external photons couple to the light quark loop.

The explicit results for $C_{\gamma\gamma H}^{(\text{non-sing})}$ and $C_{\gamma\gamma H}^{(\text{sing})}$ are presented along with the two-loop results in Appendix A, both for an on-shell and an $\overline{\text{MS}}$ -renormalized massive quark mass. In addition, we provide them in electronic form in an ancillary file, see Appendix C. The $\overline{\text{MS}}$ -renormalized result, expanded around $x = 1$ up to the order $\mathcal{O}((1-x)^{40})$, agrees with Ref. [24].

Fig. 2 shows the real and imaginary part of the three-loop amplitude, separately for the singlet and the non-singlet component.

3.2 Results for C_{ggH}

The form factor C_{ggH} can also be written as a series in α_s ,

$$C_{ggH} = \frac{1}{v} \frac{\alpha_s}{\pi} \left[C_{ggH}^{(0)} + \frac{\alpha_s}{\pi} C_{ggH}^{(1)} + \left(\frac{\alpha_s}{\pi} \right)^2 C_{ggH}^{(2)} + \mathcal{O}(\alpha_s^3) \right]. \quad (3.4)$$

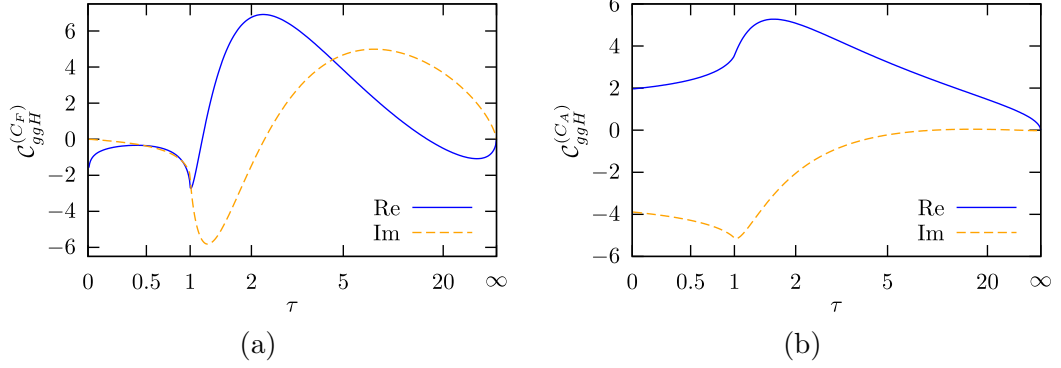


Figure 3: Contributions to $\tilde{C}_{ggH}^{(2)}$ separated by their color factors. The quark mass is renormalized in the on-shell scheme and the renormalization scale is set to $\mu^2 = M_H^2$.

We provide again the one-loop result to fix the notation,

$$C_{ggH}^{(0)} = T_F \left[-\frac{4x}{(1-x)^2} + \frac{2x(1+x)^2}{(1-x)^4} H_{0,0} \right]. \quad (3.5)$$

In contrast to the $C_{\gamma\gamma H}$ form factor, the purely virtual ggH result is not finite after the ultraviolet renormalization procedure. This is due to infrared divergences which cancel against real corrections, or are absorbed into PDFs. In Ref. [51] it is shown that the structure of these infrared divergences is universal and can be subtracted:

$$\tilde{C}_{ggH}^{(1)} = C_{ggH}^{(1)} - \frac{1}{2} I_g^{(1)} C_{ggH}^{(0)}, \quad (3.6a)$$

$$\tilde{C}_{ggH}^{(2)} = C_{ggH}^{(2)} - \frac{1}{2} I_g^{(1)} C_{ggH}^{(1)} - \frac{1}{4} I_g^{(2)} C_{ggH}^{(0)}. \quad (3.6b)$$

The factors $I_g^{(1)}$ and $I_g^{(2)}$ are given by [51, 52]

$$I_g^{(1)} \equiv I_g^{(1)}(\epsilon) = - \left(-\frac{\mu^2}{M_H^2} \right)^\epsilon \frac{e^{\epsilon\gamma_E}}{\Gamma(1-\epsilon)} \left[\frac{C_A}{\epsilon^2} + \frac{\beta_0}{\epsilon} \right], \quad (3.7a)$$

$$I_g^{(2)} = -\frac{1}{2} I_g^{(1)}(\epsilon) \left(I_g^{(1)}(\epsilon) + \frac{\beta_0}{\epsilon} \right) + \frac{e^{-\epsilon\gamma_E} \Gamma(1-2\epsilon)}{\Gamma(1-\epsilon)} \left(\frac{\beta_0}{\epsilon} + K \right) I_g^{(1)}(2\epsilon) + \frac{e^{\epsilon\gamma_E}}{\Gamma(1-\epsilon)} \frac{H_g}{2\epsilon}, \quad (3.7b)$$

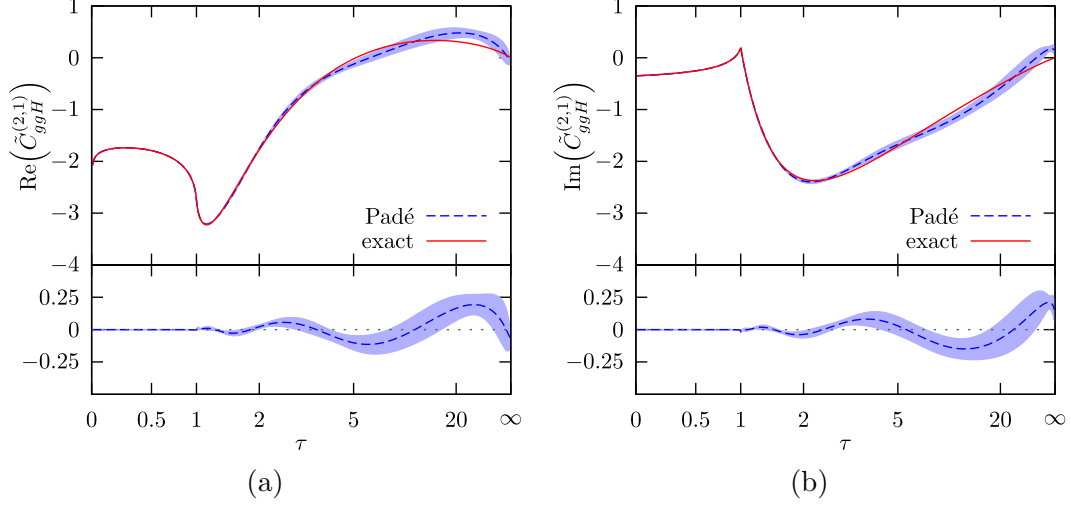


Figure 4: Real and imaginary part of $\tilde{C}_{ggH}^{(2,1)}$ with the quark mass renormalized on-shell, $\mu^2 = -M_H^2$, and the color factors set to their $SU(3)$ values. The red (solid) line is the result given in eqs. (3.10,B.4,B.5). The blue (dashed) line shows the Padé approximation found in Ref. [28]; the associated uncertainty estimate is indicated by the blue shaded band. The lower panel shows the difference between the Padé approximation and our result.

and

$$\beta_0 = \frac{11}{6}C_A - \frac{2}{3}T_F n_l, \quad (3.8a)$$

$$K = \left(\frac{67}{18} - \frac{\pi^2}{6} \right) C_A - \frac{10}{9}T_F n_l, \quad (3.8b)$$

$$H_g = \frac{20}{27}T_F^2 n_l^2 + T_F C_F n_l - \left(\frac{\pi^2}{36} + \frac{58}{27} \right) T_F n_l C_A + \left(\frac{\zeta_3}{2} + \frac{5}{12} + \frac{11\pi^2}{144} \right) C_A^2. \quad (3.8c)$$

The finite three-loop terms can be parameterized as

$$\tilde{C}_{ggH}^{(2)} = \tilde{C}_{ggH}^{(2,0)} + n_l \tilde{C}_{ggH}^{(2,1)} + n_l^2 \tilde{C}_{ggH}^{(2,2)}, \quad (3.9)$$

where $\tilde{C}_{ggH}^{(2,0)}$ denotes the contribution of Feynman diagrams without a light quark loop. Since at the three-loop level there are no diagrams with more than two closed quark loops, the $\tilde{C}_{ggH}^{(2,2)}$ contribution originates solely from the subtraction terms of eq. (3.6b). We further decompose $\tilde{C}_{ggH}^{(2,1)}$ into its contributions to different color factors,

$$\tilde{C}_{ggH}^{(2,1)} = T_F^2 C_F \mathcal{C}_{ggH}^{(C_F)} + T_F^2 C_A \mathcal{C}_{ggH}^{(C_A)}. \quad (3.10)$$

Explicit results for $\mathcal{C}_{ggH}^{(C_F)}$ and $\mathcal{C}_{ggH}^{(C_A)}$, where the quark mass again has been renormalized both in the $\overline{\text{MS}}$ and the on-shell scheme, are given along with the two-loop results in Appendix B and in an ancillary file, see Appendix C. The result renormalized in the on-shell scheme, expanded around $x = 1$ up to $\mathcal{O}((1-x)^{12})$, agrees with Refs. [5, 26, 28]. Also all terms of the threshold expansion given in Refs. [27, 28] could be reproduced. The real and imaginary part of the result is shown in fig. 3.

Fig. 4 compares these results to the semi-numerical approximation of Ref. [28].³ The latter is associated with a systematic uncertainty due to the approximation procedure, which is dominated at large τ by the absence of any input from this kinematical region into the Padé approximants. Our results indeed confirm the associated uncertainty estimate for the light-quark terms up to rather large values of τ (corresponding to large Higgs masses/virtualities or small quark masses).

4 Conclusions

The Higgs-gluon form factor is an essential component for the theoretical description of Higgs physics at hadron colliders. It enters the total cross section for single and double Higgs production at the LHC, for example. In QCD, it involves a massive quark loop which mediates the Higgs-gluon/photon coupling. Until recently, the three-loop ggH form factor has been known only in the limit of a very heavy mediating quark. This has restricted its applicability to top-quark mediated on-shell (or not-too off-shell) single production of the SM-like Higgs boson. Even there, the lack of an exact result implied non-negligible uncertainties. In cases such as double-Higgs production, off-shell or bottom-quark mediated single-Higgs production, or the production of heavy beyond-the-SM (BSM) Higgs bosons, the expansion fails and one had to resort to the NLO result.

In this paper, we provided an analytic three-loop result for the component of the gluon-Higgs form factor which, in addition to the massive quark loop, involves a closed massless quark loop. We showed that it can be computed in closed form for a general quark mass, and presented it in terms of harmonic polylogarithms. Comparison of this result to a recent semi-numerical evaluation of the full Higgs-gluon form factor shows very good agreement at the level of the estimated numerical uncertainties. As a byproduct of our calculation, we also presented the analogous component of the amplitude for the decay rate of the Higgs boson into photons.

A large portion of our technical setup is applicable also to the full form factor. However, the calculations are much more expensive than for the light-quark terms considered here.

³ In accordance with Ref. [28], we set $\mu^2 = -M_H^2$ in fig. 4.

Moreover, one encounters elliptic integrals which cannot be expressed in terms of harmonic polylogarithms. A fully analytical result for the three-loop form factor therefore requires further efforts.

Acknowledgments. We would like to thank Florian Herren and Philipp Maierhöfer for helpful discussions, and Matthias Steinhauser for useful comments on the manuscript. This work was supported by Deutsche Forschungsgemeinschaft (DFG) through the Collaborative Research Center TRR 257 “Particle Physics Phenomenology after the Higgs Discovery”. J.U. received funding from the European Research Council (ERC) under the European Unions Horizon 2020 research and innovation programme under grant agreement no. 647356 (CutLoops). The authors acknowledge support by the state of Baden-Württemberg through bwHPC and the German Research Foundation (DFG) through grant no INST 39/963-1 FUGG. Parts of the computing resources were granted by RWTH Aachen University under project rwth0119. We would also like to thank Peter Uwer and his group “Phenomenology of Elementary Particle Physics beyond the Standard Model” at Humboldt-Universität zu Berlin for providing computer resources. The Feynman diagrams in this article have been drawn with *JaxoDraw* [53] based on *Axodraw* [54].

A Results for $C_{\gamma\gamma H}$

In this appendix, we provide explicit formulas for the two-loop result and the newly computed light-quark contributions to the three-loop result of the $\gamma\gamma H$ form factor, cf. eqs. (3.1,3.3). We use $H_{\vec{a}} \equiv H(\vec{a}; x)$ to denote harmonic polylogarithms [55, 56], $\zeta_n \equiv \sum_{j=1}^{\infty} j^{-n}$ for Riemann’s zeta function, and the short-hand notation $L_{\mu} \equiv \ln(\mu^2/m_q^2)$ with the renormalization scale μ .

The two-loop result has been known for about 15 years [22]. In our notation, it reads

$$\begin{aligned}
C_{\gamma\gamma H}^{(1)} = \frac{C_A C_F Q_q^2}{T_F} \Big\{ & -\frac{5x}{(1-x)^2} + \frac{x(1-14x+x^2)}{(1-x)^4} \zeta_3 - \frac{3x(1+x)}{(1-x)^3} H_0 + \frac{6x^2}{(1-x)^4} H_{0,0} \\
& - \frac{x(5-6x+5x^2)}{(1-x)^4} H_{1,0,0} + \frac{x(3+25x-7x^2+3x^3)}{2(1-x)^5} H_{0,0,0} \\
& + \frac{x(1+x)^2}{6(1-x)^4} \left[-\pi^2 H_0 - 24H_{0,-1,0} + 6H_{0,1,0} \right] + \frac{x(1+x)(1+x^2)}{60(1-x)^5} \\
& \times \left[-3\pi^4 - 20\pi^2 H_{0,0} + 240H_{0,-1,0,0} - 480H_{0,0,-1,0} - 30H_{0,0,0,0} \right. \\
& \left. + 120H_{0,0,1,0} - 420H_{0,1,0,0} - 240H_0 \zeta_3 \right] \Big\}, \tag{A.1}
\end{aligned}$$

$$\overline{C}_{\gamma\gamma H}^{(1)} = C_{\gamma\gamma H}^{(1)} + \Delta C_{\gamma\gamma H}^{(1)}, \quad (\text{A.2})$$

$$\Delta C_{\gamma\gamma H}^{(1)} = \frac{C_A C_F Q_q^2}{T_F} \left\{ \frac{x}{(1-x)^2} \left[-4 - 3L_\mu \right] + \frac{x(1+x)}{2(1-x)^3} \left[4H_0 + 3H_{0,L_\mu} \right] \right. \\ \left. + \frac{x(1+6x+x^2)}{2(1-x)^4} \left[4H_{0,0} + 3H_{0,0,L_\mu} \right] \right\}, \quad (\text{A.3})$$

where $C_{\gamma\gamma H}^{(1)}$ ($\overline{C}_{\gamma\gamma H}^{(1)}$) is the result for a quark mass renormalized in the on-shell ($\overline{\text{MS}}$) scheme. At three loops, the non-singlet contribution, with the quark mass renormalized in the on-shell scheme, is given by

$$\begin{aligned} \mathcal{C}_{\gamma\gamma H}^{(\text{non-sing})} = & -\frac{(5-7x)x}{18(1-x)^3} \pi^2 - \frac{x(1-14x+x^2)}{3(1-x)^4} L_\mu \zeta_3 + \frac{x(13+118x+13x^2)}{9(1-x)^4} \zeta_3 \\ & + \frac{x(63-85x+73x^2+21x^3)}{1080(1-x)^5} \pi^4 - \frac{4x(1-4x+x^2)}{3(1-x)^4} H_1 \zeta_3 + \frac{x(17+10x-x^2)}{54(1-x)^4} \\ & \times \pi^2 H_0 + \frac{2x(16+19x-20x^2+13x^3)}{9(1-x)^5} H_0 \zeta_3 - \frac{2x^2}{(1-x)^4} H_{0,0} L_\mu \\ & + \frac{x(3-14x-10x^2)}{3(1-x)^4} H_{0,0} + \frac{x(47+95x-115x^2+5x^3)}{108(1-x)^5} \pi^2 H_{0,0} \\ & - \frac{2x(7+29x+7x^2)}{9(1-x)^4} H_{0,1,0} - \frac{x(33+499x-265x^2-99x^3)}{36(1-x)^5} H_{0,0,0} \\ & - \frac{x(3+25x-7x^2+3x^3)}{6(1-x)^5} H_{0,0,0} L_\mu + \frac{4x(11+34x+11x^2)}{9(1-x)^4} H_{0,-1,0} \\ & - \frac{2x(3-2x+3x^2)}{3(1-x)^4} H_{1,1,0,0} - \frac{x(2+62x+17x^2+17x^3)}{9(1-x)^5} H_{0,0,0,0} \\ & - \frac{x(47+119x-67x^2+29x^3)}{18(1-x)^5} H_{0,0,1,0} + \frac{8x(1+x)(2+6x-7x^2)}{9(1-x)^5} H_{0,-1,0,0} \\ & + \frac{x(17-42x+17x^2)}{6(1-x)^4} H_{1,0,0,0} + \frac{4x(19+31x-23x^2+13x^3)}{9(1-x)^5} H_{0,0,-1,0} \\ & + \frac{2x(10-11x-11x^2+34x^3)}{9(1-x)^5} H_{0,1,0,0} + \frac{x(1+x)}{6(1-x)^3} \left[23H_0 - 16H_{-1,0} + 10H_{1,0} \right. \\ & \left. + 6H_0 L_\mu \right] + \frac{x(5-6x+5x^2)}{9(1-x)^4} \left[5H_{1,0,0} + 3H_{1,0,0} L_\mu \right] + \frac{x}{18(1-x)^2} \left[101 \right. \\ & \left. - \pi^2 H_{1,0} - 96H_{1,0,-1,0} + 42H_{1,0,1,0} + 30L_\mu \right] + \frac{x(1+x)^2}{18(1-x)^4} \left[2\pi^2 H_{0,1} \right. \\ & \left. - 96H_{0,-1,-1,0} + 48H_{0,-1,1,0} + 48H_{0,1,-1,0} - 12H_{0,1,1,0} + \pi^2 H_0 L_\mu - 6H_{0,1,0} L_\mu \right] \end{aligned}$$

$$\begin{aligned}
& + 24H_{0,-1,0}L_\mu \Big] + \frac{x(1+x)(1+x^2)}{540(1-x)^5} \Big[-18\pi^4 H_{-1} + 14\pi^4 H_0 - 120\pi^2 H_{-1,0,0} \\
& + 120\pi^2 H_{0,0,0} + 120\pi^2 H_{0,0,1} + 1440H_{-1,0,-1,0,0} - 2880H_{-1,0,0,-1,0} + 9\pi^4 L_\mu \\
& - 180H_{-1,0,0,0,0} + 720H_{-1,0,0,1,0} - 2520H_{-1,0,1,0,0} + 1440H_{0,-1,-1,0,0} - 30\pi^2 \zeta_3 \\
& + 1440H_{0,-1,0,-1,0} - 1800H_{0,-1,0,0,0} - 720H_{0,-1,0,1,0} - 5760H_{0,0,-1,-1,0} \\
& + 2880H_{0,0,-1,0,0} + 2880H_{0,0,-1,1,0} + 2880H_{0,0,0,-1,0} + 270H_{0,0,0,0,0} + 2520\zeta_5 \\
& - 720H_{0,0,0,1,0} + 2880H_{0,0,1,-1,0} - 720H_{0,0,1,0,0} - 720H_{0,0,1,1,0} + 3060H_{0,1,0,0,0} \\
& - 4320H_{0,1,0,-1,0} + 2160H_{0,1,0,1,0} - 360H_{0,1,1,0,0} + 60\pi^2 H_{0,0}L_\mu + 90H_{0,0,0,0}L_\mu \\
& - 720H_{0,-1,0,0}L_\mu + 1440H_{0,0,-1,0}L_\mu - 360H_{0,0,1,0}L_\mu + 1260H_{0,1,0,0}L_\mu \\
& - 1440H_{-1,0}\zeta_3 - 360H_{0,-1}\zeta_3 + 1080H_{0,0}\zeta_3 - 1800H_{0,1}\zeta_3 + 720H_0L_\mu\zeta_3 \Big].
\end{aligned} \tag{A.4}$$

The singlet contribution is

$$\begin{aligned}
\mathcal{C}_{\gamma\gamma H}^{(\text{sing})} = & -\frac{x(37-243x+249x^2-15x^3)}{6(1-x)^5}\zeta_3 + \frac{5x(1-22x+x^2)}{3(1-x)^4}\zeta_5 \\
& + \frac{x(3+44x-68x^2+20x^3+15x^4)}{1080(1-x)^6}\pi^4 - \frac{39x^2}{2(1-x)^3}H_0 - \frac{x^2(4-x+11x^2)}{18(1-x)^5}\pi^2 H_0 \\
& + \frac{3x}{2(1-x)^2}\left[2+13H_1\right] + \frac{4x(1+3x+x^2)}{(1-x)^4}H_1\zeta_3 + \frac{2x^2(14-20x-4x^2+3x^3)}{3(1-x)^6} \\
& \times H_0\zeta_3 - \frac{4x(1+8x+x^2)}{3(1-x)^4}H_{1,0}\zeta_3 + \frac{x^2(35+66x)}{6(1-x)^4}H_{0,0} + \frac{x^2(2-5x+2x^2-6x^3)}{9(1-x)^6} \\
& \times \pi^2 H_{0,0} - \frac{x^2(22-145x-7x^2)}{6(1-x)^5}H_{0,0,0} - \frac{2x(1-x+x^2)}{9(1-x)^4}\pi^2 H_{1,0,0} \\
& + \frac{x(13-266x+13x^2)}{6(1-x)^4}H_{1,0,0} + \frac{2x(4-22x+25x^2+7x^3)}{3(1-x)^5}H_{0,-1,0} \\
& + \frac{x(1-3x+9x^2+21x^3)}{3(1-x)^5}H_{0,0,1} - \frac{2x(1+2x-7x^2)}{(1-x)^5}H_{0,1,0,0} - \frac{2x(1+10x+x^2)}{(1-x)^4} \\
& \times H_{1,1,0,0} + \frac{2x^2(1+3x)}{(1-x)^5}H_{0,0,1,0} + \frac{2x(1-6x-2x^2)}{(1-x)^4}H_{1,0,0,0} \\
& + \frac{x^2(2+7x-10x^2-6x^3)}{3(1-x)^6}H_{0,0,0,0} + \frac{x(1-10x+x^2)}{(1-x)^4}H_{0,1,0,0,0} + \frac{x(1+x)}{36(1-x)^3} \\
& \times \left[-7\pi^2 + 444H_{-1,0} + 156H_{0,1} - 108H_{1,0}\right] + \frac{x(1+x)(11-8x+11x^2)}{18(1-x)^5}\left[\pi^2 H_{-1} \right. \\
& \left. - 12H_{-1,-1,0} - 12H_{-1,0,1}\right] + \frac{x(1+x^2)}{3(1-x)^4}\left[12H_{1,0,-1,0} + 12H_{1,0,0,1} + \pi^2 \zeta_3\right]
\end{aligned}$$

$$\begin{aligned}
& + \frac{4x^2(1+11x-11x^2+6x^3)}{3(1-x)^6} [H_{0,0,-1,0} + H_{0,0,0,1}] \\
& + \frac{x(3-4x+16x^2-4x^3+3x^4)}{9(1-x)^6} [\pi^2 H_{0,-1} - 12H_{0,-1,-1,0} - 12H_{0,-1,0,1}] \\
& + \frac{x(1-4x+x^2)}{270(1-x)^4} [\pi^4 H_1 - 270H_{0,1,0} + 720H_{1,0,0,-1,0} + 720H_{1,0,0,0,1}] + \frac{x(1+x)^2}{9(1-x)^4} \\
& \times \left[-3\pi^2 H_{1,0} + 2\pi^2 H_{0,0,-1} + 4\pi^2 H_{1,0,-1} - 24H_{0,0,-1,-1,0} - 24H_{0,0,-1,0,1} \right. \\
& \quad - 3H_{0,0,1,0,0} - 48H_{1,0,-1,-1,0} - 48H_{1,0,-1,0,1} - 6H_{1,0,0,0,0} \Big] + \frac{2x^2}{3(1-x)^4} \left[\pi^2 H_{0,1,0} \right. \\
& \quad + 2\pi^2 H_{1,1,0} - 6H_{1,0,1,0} - 24H_{0,1,0,-1,0} - 24H_{0,1,0,0,1} - 6H_{0,1,0,1,0} - 12H_{0,1,1,0,0} \\
& \quad - 6H_{1,0,0,1,0} - 12H_{1,0,1,0,0} - 48H_{1,1,0,-1,0} - 18H_{1,1,0,0,0} - 48H_{1,1,0,0,1} \\
& \quad \left. - 12H_{1,1,0,1,0} - 12H_{0,1}\zeta_3 - 24H_{1,1,1,0,0} - 24H_{1,1}\zeta_3 \right]. \tag{A.5}
\end{aligned}$$

The results with an $\overline{\text{MS}}$ renormalized quark mass can be written as

$$\overline{\mathcal{C}}_{\gamma\gamma H}^{(\text{non-sing})} = \mathcal{C}_{\gamma\gamma H}^{(\text{non-sing})} + \Delta\mathcal{C}_{\gamma\gamma H}^{(\text{non-sing})} \tag{A.6}$$

$$\overline{\mathcal{C}}_{\gamma\gamma H}^{(\text{sing})} = \mathcal{C}_{\gamma\gamma H}^{(\text{sing})}, \tag{A.7}$$

where

$$\begin{aligned}
\Delta\mathcal{C}_{\gamma\gamma H}^{(\text{non-sing})} = & \frac{x}{24(1-x)^2} \left[71 + 8\pi^2 + 52L_\mu + 12L_\mu^2 \right] + \frac{x(1+x)}{48(1-x)^3} \left[-71H_0 - 8\pi^2 H_0 \right. \\
& \left. - 52H_0 L_\mu - 12H_0 L_\mu^2 \right] + \frac{x(1+6x+x^2)}{48(1-x)^4} \left[-71H_{0,0} - 8\pi^2 H_{0,0} - 52H_{0,0} L_\mu \right. \\
& \left. - 12H_{0,0} L_\mu^2 \right]. \tag{A.8}
\end{aligned}$$

Note that the singlet component appears for the first time at the three-loop order and is therefore renormalization scheme independent.

B Results for C_{ggH}

In this appendix, we provide explicit formulas for the two-loop and the newly computed light-quark contribution to the three-loop result of the ggH form factor, cf. eqs. (3.4,3.10). The notation is the same as in Appendix A.

Again, the two-loop result has been known for about 15 years [19–21]. In our notation, it reads

$$\begin{aligned}
\tilde{C}_{ggH}^{(1)} = & T_F C_A \left\{ \frac{2x(3+x)(1+3x)}{(1-x)^4} \zeta_3 + \frac{x}{3(1-x)^2} \left[-18 - 11H_0 - 22H_1 - 11L_\mu \right] \right. \\
& - \frac{x(7+38x+7x^2)}{3(1-x)^4} H_{1,0,0} + \frac{x(11+15x+21x^2+x^3)}{2(1-x)^5} H_{0,0,0} + \frac{x(1+x)^2}{90(1-x)^4} \\
& \times \left[8\pi^4 + 90H_{0,0} + 30\pi^2 H_{0,0} + 60\pi^2 H_{1,0} + 330H_{0,0,1} + 330H_{0,1,0} \right. \\
& + 90H_{0,0,0,0} + 360H_{0,0,-1,0} + 720H_{1,0,-1,0} - 360H_{1,0,0,0} + 165H_{0,0} L_\mu \\
& \left. \left. + 540H_0 \zeta_3 + 1080H_1 \zeta_3 \right] \right\} \\
& + T_F C_F \left\{ -\frac{10x}{(1-x)^2} + \frac{2x(1-14x+x^2)}{(1-x)^4} \zeta_3 - \frac{6x(1+x)}{(1-x)^3} H_0 + \frac{12x^2}{(1-x)^4} H_{0,0} \right. \\
& - \frac{2x(5-6x+5x^2)}{(1-x)^4} H_{1,0,0} + \frac{x(3+25x-7x^2+3x^3)}{(1-x)^5} H_{0,0,0} \\
& + \frac{x(1+x)^2}{3(1-x)^4} \left[-\pi^2 H_0 - 24H_{0,-1,0} + 6H_{0,1,0} \right] + \frac{x(1+x)(1+x^2)}{30(1-x)^5} \left[-3\pi^4 \right. \\
& - 20\pi^2 H_{0,0} + 240H_{0,-1,0,0} - 480H_{0,0,-1,0} - 30H_{0,0,0,0} + 120H_{0,0,1,0} \\
& \left. \left. - 420H_{0,1,0,0} - 240H_0 \zeta_3 \right] \right\} \\
& + n_l T_F^2 \left\{ \frac{4x}{3(1-x)^2} \left[H_0 + 2H_1 + L_\mu \right] + \frac{2x(1+x)^2}{3(1-x)^4} \left[-3H_{0,0,0} - 2H_{0,0,1} - 2H_{0,1,0} \right. \right. \\
& \left. \left. - 2H_{1,0,0} - H_{0,0} L_\mu \right] \right\}, \tag{B.1}
\end{aligned}$$

$$\bar{\tilde{C}}_{ggH}^{(1)} = \tilde{C}_{ggH}^{(1)} + \Delta \tilde{C}_{ggH}^{(1)}, \tag{B.2}$$

$$\begin{aligned}
\Delta \tilde{C}_{ggH}^{(1)} = & T_F C_F \left\{ \frac{2x}{(1-x)^2} \left[-4 - 3L_\mu \right] + \frac{x(1+x)}{(1-x)^3} \left[4H_0 + 3H_0 L_\mu \right] \right. \\
& \left. + \frac{x(1+6x+x^2)}{(1-x)^4} \left[4H_{0,0} + 3H_{0,0} L_\mu \right] \right\}, \tag{B.3}
\end{aligned}$$

where again the symbols with (without) a bar on top denote the results for an $\overline{\text{MS}}$ (on-shell) renormalized quark mass.

The contribution to the three-loop ggH form factor proportional to the color factor C_F , cf. eq. (3.10), is given by

$$\mathcal{C}_{ggH}^{(C_F)} = -\frac{(17-7x)x}{18(1-x)^3} \pi^2 - \frac{4x(1-14x+x^2)}{3(1-x)^4} L_\mu \zeta_3 - \frac{x(85-939x+957x^2-19x^3)}{9(1-x)^5} \zeta_3$$

$$\begin{aligned}
& + \frac{2(1-3x)x(19-44x-3x^2)}{3(1-x)^5} \zeta_5 + \frac{(5-7x)x(1+x^2)}{9(1-x)^5} \pi^2 \zeta_3 \\
& + \frac{x(33-52x+45x^2-16x^3-3x^4)}{270(1-x)^6} \pi^4 + \frac{x}{9(1-x)^2} \left[155 + 411H_1 + 60L_\mu \right] \\
& + \frac{(33-104x)x}{3(1-x)^3} H_0 + \frac{4x(3+40x+3x^2)}{3(1-x)^4} H_1 \zeta_3 + \frac{x(17-19x-8x^2-32x^3)}{27(1-x)^5} \pi^2 H_0 \\
& + \frac{2x(5+2x+7x^2+4x^3)}{135(1-x)^5} \pi^4 H_1 + \frac{2x(29+138x-288x^2+90x^3-11x^4)}{9(1-x)^6} H_0 \zeta_3 \\
& - \frac{x(5+6x+5x^2)}{9(1-x)^4} \pi^2 H_{1,0} - \frac{4x(1+13x-11x^2+x^3)}{3(1-x)^5} H_{0,1} \zeta_3 \\
& + \frac{x(18+7x+34x^2)}{3(1-x)^4} H_{0,0} + \frac{8x(1-5x+9x^2+3x^3)}{3(1-x)^5} H_{1,0} \zeta_3 \\
& + \frac{x(59+72x-294x^2+144x^3-65x^4)}{54(1-x)^6} \pi^2 H_{0,0} + \frac{2x(3-4x+16x^2-4x^3+3x^4)}{9(1-x)^6} \\
& \times \pi^2 H_{0,-1} - \frac{2x(23+58x+23x^2)}{9(1-x)^4} H_{0,1,0} - \frac{x(33+847x-1351x^2-141x^3)}{18(1-x)^5} H_{0,0,0} \\
& - \frac{2x(3+25x-7x^2+3x^3)}{3(1-x)^5} H_{0,0,0} L_\mu + \frac{4x^2(3-x+2x^2)}{9(1-x)^5} \pi^2 H_{1,0,0} \\
& + \frac{4x(5-6x+5x^2)}{3(1-x)^4} H_{1,0,0} L_\mu + \frac{x(89-930x+89x^2)}{9(1-x)^4} H_{1,0,0} \\
& + \frac{4x(34-20x+29x^2-x^3)}{9(1-x)^5} H_{0,-1,0} + \frac{2x(1-15x+21x^2+21x^3)}{3(1-x)^5} H_{0,0,1} \\
& - \frac{x(77+245x-229x^2+35x^3)}{9(1-x)^5} H_{0,0,1,0} - \frac{2x(3+18x-76x^2+54x^3-27x^4)}{3(1-x)^6} \\
& \times H_{0,0,0,1} - \frac{2x(20+186x-258x^2+90x^3-17x^4)}{9(1-x)^6} H_{0,0,0,0} \\
& - \frac{8x(1-4x+20x^2-4x^3+x^4)}{3(1-x)^6} H_{0,-1,0,1} - \frac{8x(7-4x+8x^2-4x^3+7x^4)}{3(1-x)^6} \\
& \times H_{0,-1,-1,0} + \frac{16x(1+x)(5+6x-10x^2)}{9(1-x)^5} H_{0,-1,0,0} + \frac{16x(1-10x+x^2)}{3(1-x)^4} H_{1,1,0,0} \\
& + \frac{8x(1+12x+x^2)}{3(1-x)^4} H_{1,0,-1,0} + \frac{2x(5-14x+5x^2)}{(1-x)^4} H_{1,0,1,0} + \frac{4x(11-6x+11x^2)}{3(1-x)^4} \\
& \times H_{1,0,0,1} + \frac{x(53-259x+187x^2-29x^3)}{3(1-x)^5} H_{1,0,0,0} + \frac{4x(1-86x+82x^2+25x^3)}{9(1-x)^5}
\end{aligned}$$

$$\begin{aligned}
& \times H_{0,1,0,0} + \frac{8x(25 + 15x - 33x^2 + 3x^3 + 11x^4)}{9(1-x)^6} H_{0,0,-1,0} - \frac{2x(1+x)(1-3x^2)}{3(1-x)^5} \\
& \times H_{1,0,0,0} - \frac{16x(1+x)(5+3x^2)}{3(1-x)^5} H_{0,0,-1,-1,0} - \frac{16x(1+7x-5x^2+x^3)}{3(1-x)^5} H_{0,1,0,-1,0} \\
& + \frac{16x(1-4x+x^2)}{3(1-x)^4} H_{1,0,0,0,1} + \frac{16x(1+x)(1+3x^2)}{3(1-x)^5} H_{0,0,-1,0,1} \\
& + \frac{4x(1+x)(3+4x^2)}{3(1-x)^5} H_{0,0,1,0,0} + \frac{16x(3-3x+7x^2+x^3)}{3(1-x)^5} H_{1,0,0,-1,0} \\
& + \frac{4x(7+x+12x^2+6x^3)}{(1-x)^5} H_{0,1,0,0,0} + \frac{4x(7-5x+19x^2+7x^3)}{3(1-x)^5} H_{1,0,1,0,0} \\
& + \frac{4x(7-17x+31x^2+7x^3)}{3(1-x)^5} H_{0,1,0,0,1} + \frac{4x(11+5x+17x^2+11x^3)}{3(1-x)^5} H_{0,1,0,1,0} \\
& + \frac{4x(13+x+25x^2+13x^3)}{3(1-x)^5} H_{0,1,1,0,0} + \frac{2x(1+x)}{3(1-x)^3} \left[29H_{-1,0} + 19H_{0,1} + 2H_{1,0} \right. \\
& \quad \left. + 6H_0 L_\mu \right] + \frac{x(1+x)(11-8x+11x^2)}{9(1-x)^5} \left[\pi^2 H_{-1} - 12H_{-1,-1,0} - 12H_{-1,0,1} \right] \\
& + \frac{4x(1+4x-2x^2+x^3)}{9(1-x)^5} \left[\pi^2 H_{0,1,0} - 6H_{1,0,0,1,0} \right] + \frac{8x^2}{3(1-x)^4} \left[\pi^2 H_{1,1,0} - 9H_{1,1,0,0,0} \right. \\
& \quad \left. - 24H_{1,1,0,-1,0} - 24H_{1,1,0,0,1} - 6H_{1,1,0,1,0} - 12H_{1,1,1,0,0} - 3H_{0,0} L_\mu - 12H_{1,1} \zeta_3 \right] \\
& + \frac{2x(1+x)^2}{9(1-x)^4} \left[2\pi^2 H_{0,1} + 2\pi^2 H_{0,0,-1} + 4\pi^2 H_{1,0,-1} + 48H_{0,-1,1,0} + 48H_{0,1,-1,0} \right. \\
& \quad \left. - 6H_{0,1,0,1} - 18H_{0,1,1,0} - 48H_{1,0,-1,-1,0} - 48H_{1,0,-1,0,1} + \pi^2 H_0 L_\mu + 24H_{0,-1,0} L_\mu \right. \\
& \quad \left. - 6H_{0,1,0} L_\mu \right] + \frac{x(1+x)(1+x^2)}{270(1-x)^5} \left[-18\pi^4 H_{-1} + 23\pi^4 H_0 - 120\pi^2 H_{-1,0,0} \right. \\
& \quad + 300\pi^2 H_{0,0,0} + 240\pi^2 H_{0,0,1} + 1440H_{-1,0,-1,0,0} - 2880H_{-1,0,0,-1,0} + 720H_{0,0,0,0,0} \\
& \quad - 180H_{-1,0,0,0,0} + 720H_{-1,0,0,1,0} - 2520H_{-1,0,1,0,0} + 1440H_{0,-1,-1,0,0} + 18\pi^4 L_\mu \\
& \quad + 1440H_{0,-1,0,-1,0} - 3960H_{0,-1,0,0,0} - 1440H_{0,-1,0,0,1} - 2160H_{0,-1,0,1,0} \\
& \quad - 1440H_{0,-1,1,0,0} + 4320H_{0,0,-1,0,0} + 5760H_{0,0,-1,1,0} + 7200H_{0,0,0,-1,0} \\
& \quad + 180H_{0,0,0,0,1} - 1620H_{0,0,0,1,0} + 5760H_{0,0,1,-1,0} - 720H_{0,0,1,0,1} - 2160H_{0,0,1,1,0} \\
& \quad - 1440H_{0,1,-1,0,0} - 1440H_{1,0,-1,0,0} + 120\pi^2 H_{0,0} L_\mu - 1440H_{0,-1,0,0} L_\mu \\
& \quad + 2880H_{0,0,-1,0} L_\mu + 180H_{0,0,0,0} L_\mu - 720H_{0,0,1,0} L_\mu + 2520H_{0,1,0,0} L_\mu \\
& \quad \left. - 1440H_{-1,0} \zeta_3 - 360H_{0,-1} \zeta_3 + 2520H_{0,0} \zeta_3 + 1440H_0 L_\mu \zeta_3 \right], \tag{B.4}
\end{aligned}$$

where the quark mass has been renormalized in the on-shell scheme. The contribution

proportional to the color factor C_A is given by

$$\begin{aligned}
\mathcal{C}_{ggH}^{(C_A)} = & -\frac{4x(3+x)(1+3x)}{3(1-x)^4}L_\mu\zeta_3 - \frac{x(79+193x-202x^2-112x^3)}{9(1-x)^5}\zeta_3 \\
& - \frac{x(283-708x+460x^2-420x^3+427x^4)}{3240(1-x)^6}\pi^4 + \frac{(17-77x)x}{216(1-x)^3}\pi^2 \\
& - \frac{x(1-27x+21x^2-23x^3)}{36(1-x)^5}\pi^2 H_0 - \frac{x(25-8x-84x^2+16x^3+37x^4)}{3(1-x)^6}H_0\zeta_3 \\
& + \frac{(422-485x)x}{54(1-x)^3}H_0 - \frac{x(25+38x+25x^2)}{27(1-x)^4}\pi^2 H_{1,0} \\
& - \frac{x(127-96x-686x^2+96x^3+223x^4)}{432(1-x)^6}\pi^2 H_{0,0} + \frac{(85-91x)x}{9(1-x)^3}H_{1,0} \\
& + \frac{(97-79x)x}{9(1-x)^3}H_{0,1} + \frac{x(1+x)}{(1-x)^3}H_{-1,0} + \frac{x(1145-4208x+1253x^2)}{324(1-x)^4}H_{0,0} \\
& - \frac{2x(74+139x+74x^2)}{27(1-x)^4}H_{0,1,0} - \frac{2x(65+191x-164x^2+34x^3)}{27(1-x)^5}H_{0,0,1} \\
& - \frac{x(130+306x+225x^2+113x^3)}{18(1-x)^5}H_{0,0,0} + \frac{x(541+854x+541x^2)}{54(1-x)^4}H_{1,0,0} \\
& + \frac{2x(1-13x+10x^2-12x^3)}{3(1-x)^5}H_{0,-1,0} - \frac{x(23+50x+23x^2)}{3(1-x)^4}H_{0,1,0,0} \\
& - \frac{4x(25+86x+25x^2)}{9(1-x)^4}H_{1,0,-1,0} - \frac{4x(11+x-8x^2-5x^3+8x^4)}{3(1-x)^6}H_{0,0,0,1} \\
& - \frac{x(137+36x-7x^2-204x^3+17x^4)}{9(1-x)^6}H_{0,0,0,0} \\
& - \frac{4x(5-12x-37x^2+36x^3+29x^4)}{9(1-x)^6}H_{0,0,-1,0} + \frac{2x(19+26x+19x^2)}{9(1-x)^4}H_{1,1,0,0} \\
& + \frac{x(35+107x-215x^2-71x^3)}{9(1-x)^5}H_{1,0,0,0} + \frac{x}{324(1-x)^2}\left[3002+5442H_1+18\pi^2H_1\right. \\
& \quad \left.+6336H_{1,1}+2532L_\mu+9\pi^2L_\mu+1584H_0L_\mu+3168H_1L_\mu+792L_\mu^2\right] \\
& + \frac{8x(1-4x+x^2)}{9(1-x)^4}\left[-2H_{1,0,1,0}-H_{1,0,0}L_\mu\right] + \frac{x(1+x)(11-8x+11x^2)}{18(1-x)^5} \\
& \times \left[-\pi^2H_{-1}+12H_{-1,-1,0}+12H_{-1,0,1}\right] + \frac{2x(11+13x+5x^2-5x^3)}{3(1-x)^5}\left[-2H_{0,0,1,0}\right. \\
& \quad \left.-H_{0,0,0}L_\mu\right] + \frac{x(3-4x+16x^2-4x^3+3x^4)}{9(1-x)^6}\left[-\pi^2H_{0,-1}+12H_{0,-1,-1,0}\right.
\end{aligned}$$

$$\begin{aligned}
& + 12H_{0,-1,0,1} \Big] + \frac{x(1+x)^2}{1080(1-x)^4} \Big[-86\pi^4 H_0 - 220\pi^4 H_1 - 240\pi^2 H_{0,0,-1} - 64\pi^4 L_\mu \\
& - 585\pi^2 H_{0,0,0} - 510\pi^2 H_{0,0,1} - 1230\pi^2 H_{0,1,0} - 480\pi^2 H_{1,0,-1} - 1470\pi^2 H_{1,0,0} \\
& - 960\pi^2 H_{1,0,1} - 2400\pi^2 H_{1,1,0} - 10560H_{0,0,1,1} - 10560H_{0,1,0,1} - 10560H_{0,1,1,0} \\
& - 1920H_{1,0,0,1} + 8640H_{0,0,-1,-1,0} - 7200H_{0,0,-1,0,0} - 5760H_{0,0,-1,1,0} - 120\pi^2 \zeta_3 \\
& - 8640H_{0,0,0,-1,0} - 2880H_{0,0,0,0,0} - 2160H_{0,0,0,0,1} - 1080H_{0,0,0,1,0} + 3240H_{0,0,1,0,0} \\
& - 5760H_{0,0,1,-1,0} - 14400H_{0,1,0,-1,0} + 5040H_{0,1,0,0,0} + 17280H_{1,0,-1,-1,0} + 720\zeta_5 \\
& - 14400H_{1,0,-1,0,0} - 11520H_{1,0,-1,1,0} - 28800H_{1,0,0,-1,0} + 7920H_{1,0,0,0,0} \\
& + 5760H_{1,0,0,1,0} - 11520H_{1,0,1,-1,0} + 5760H_{1,0,1,0,0} - 28800H_{1,1,0,-1,0} \\
& + 14400H_{1,1,0,0,0} - 2780H_{0,0}L_\mu - 255\pi^2 H_{0,0}L_\mu - 480\pi^2 H_{1,0}L_\mu - 5280H_{0,0,1}L_\mu \\
& - 5280H_{0,1,0}L_\mu - 2880H_{0,0,-1,0}L_\mu - 720H_{0,0,0,0}L_\mu - 5760H_{1,0,-1,0}L_\mu \\
& + 2880H_{1,0,0,0}L_\mu - 1320H_{0,0}L_\mu^2 - 24480H_1\zeta_3 - 9750H_{0,0}\zeta_3 - 21600H_{0,1}\zeta_3 \\
& - 21600H_{1,0}\zeta_3 - 43200H_{1,1}\zeta_3 - 4320H_0L_\mu\zeta_3 - 8640H_1L_\mu\zeta_3 \Big]. \tag{B.5}
\end{aligned}$$

The results with an $\overline{\text{MS}}$ renormalized quark mass is

$$\overline{\mathcal{C}}_{ggH}^{(C_F)} = \mathcal{C}_{ggH}^{(C_F)} + \Delta\mathcal{C}_{ggH}^{(C_F)}, \tag{B.6}$$

$$\overline{\mathcal{C}}_{ggH}^{(C_A)} = \mathcal{C}_{ggH}^{(C_A)}, \tag{B.7}$$

where

$$\begin{aligned}
\Delta\mathcal{C}_{ggH}^{(C_F)} = & -\frac{x(3+11x)}{2(1-x)^3}H_0L_\mu - \frac{x(7+135x)}{24(1-x)^3}H_0 - \frac{x(11+42x+3x^2)}{2(1-x)^4}H_{0,0}L_\mu \\
& - \frac{x(135+426x+7x^2)}{24(1-x)^4}H_{0,0} + \frac{x}{12(1-x)^2} \Big[71 + 8\pi^2 + 64H_1 + 84L_\mu + 48H_1L_\mu \\
& + 36L_\mu^2 \Big] + \frac{x(1+x)}{6(1-x)^3} \Big[-2\pi^2 H_0 - 16H_{0,1} - 16H_{1,0} - 12H_{0,1}L_\mu - 12H_{1,0}L_\mu \\
& - 9H_0L_\mu^2 \Big] + \frac{x(1+6x+x^2)}{6(1-x)^4} \Big[-2\pi^2 H_{0,0} - 24H_{0,0,0} - 16H_{0,0,1} - 16H_{0,1,0} \\
& - 16H_{1,0,0} - 18H_{0,0,0}L_\mu - 12H_{0,0,1}L_\mu - 12H_{0,1,0}L_\mu - 12H_{1,0,0}L_\mu - 9H_{0,0}L_\mu^2 \Big]. \tag{B.8}
\end{aligned}$$

The contribution $\mathcal{C}_{ggH}^{(C_A)}$ is renormalization scheme independent.

For the sake of completeness, we also provide the n_t^2 -contribution $\tilde{C}_{ggH}^{(2,2)}$ originating from

the infrared subtraction, cf. eq. (3.9):

$$\begin{aligned}
\tilde{C}_{ggH}^{(2,2)} = T_F^3 \Big\{ & \frac{x}{54(1-x)^2} \Big[-\pi^2 - 40H_0 - 80H_1 - 48H_{0,0} - 96H_{0,1} - 96H_{1,0} - 192H_{1,1} \\
& - 40L_\mu - 48H_0L_\mu - 96H_1L_\mu - 24L_\mu^2 \Big] + \frac{x(1+x)^2}{108(1-x)^4} \Big[\pi^2 H_{0,0} + 120H_{0,0,0} \\
& + 80H_{0,0,1} + 80H_{0,1,0} + 80H_{1,0,0} + 288H_{0,0,0,0} + 288H_{0,0,0,1} + 288H_{0,0,1,0} \\
& + 192H_{0,0,1,1} + 288H_{0,1,0,0} + 192H_{0,1,0,1} + 192H_{0,1,1,0} + 288H_{1,0,0,0} \\
& + 192H_{1,0,0,1} + 192H_{1,0,1,0} + 192H_{1,1,0,0} + 40H_{0,0}L_\mu + 144H_{0,0,0}L_\mu \\
& + 96H_{0,0,1}L_\mu + 96H_{0,1,0}L_\mu + 96H_{1,0,0}L_\mu + 24H_{0,0}L_\mu^2 \Big] \Big\}. \tag{B.9}
\end{aligned}$$

C Ancillary File

The ancillary file `ggh-aah-nl.m` contains the main results of this paper in an electronic form readable by `Mathematica`.⁴ The following table describes its notation:

CaahOS (CaahMSbar)	$C_{\gamma\gamma H}$
CaahOS0 (CaahMSbar0)	$C_{\gamma\gamma H}^{(0)}$
CaahOS1 (CaahMSbar1)	$C_{\gamma\gamma H}^{(1)}$
CaahOS2 (CaahMSbar2)	$C_{\gamma\gamma H}^{(2)}$
caahOS2nl1nonsing (caahMSbar2nl1nonsing)	$\mathcal{C}_{\gamma\gamma H}^{(\text{non-sing})}$
caahOS2nl1sing (caahMSbar2nl1sing)	$\mathcal{C}_{\gamma\gamma H}^{(\text{sing})}$
CgghOS (CgghMSbar)	\tilde{C}_{ggH}
CgghOS0 (CgghMSbar0)	$\tilde{C}_{ggH}^{(0)}$
CgghOS1 (CgghMSbar1)	$\tilde{C}_{ggH}^{(1)}$
CgghOS2 (CgghMSbar2)	$\tilde{C}_{ggH}^{(2)}$
cgghOS2nl1cF (cgghMSbar2nl1cF)	$\mathcal{C}_{ggH}^{(C_F)}$
cgghOS2nl1cA (cgghMSbar2nl1cA)	$\mathcal{C}_{ggH}^{(C_A)}$
api	α/π

⁴Wolfram Research, Inc., *Mathematica*, Version 12.0, Champaign, IL, U.S.A.

aspi	α_s/π
Lmu	L_μ
QQ	Q_q^2
QQ2	$\sum_{i=1}^{n_l} Q_i^2$
HPL[a_List,x]	$H_{\vec{a}}$

The OS ($\overline{\text{MS}}$) versions correspond to a quark mass renormalized in the on-shell ($\overline{\text{MS}}$) scheme. The harmonic polylogarithms are in a format compatible with the `Mathematica` package `HPL.m` [56].

References

- [1] HL/HE WG2 group, M. Cepeda *et al.*, *Higgs Physics at the HL-LHC and HE-LHC*, [arXiv:1902.00134](#) [hep-ph].
- [2] M. Spira, *QCD effects in Higgs physics*, *Fortsch. Phys.* **46** (1998) 203–284, [arXiv:hep-ph/9705337](#) [hep-ph].
- [3] M. Spira, A. Djouadi, D. Graudenz, and P. M. Zerwas, *Higgs boson production at the LHC*, *Nucl. Phys.* **B453** (1995) 17–82, [arXiv:hep-ph/9504378](#) [hep-ph].
- [4] R. V. Harlander, H. Mantler, S. Marzani, and K. J. Ozeren, *Higgs production in gluon fusion at next-to-next-to-leading order QCD for finite top mass*, *Eur. Phys. J.* **C66** (2010) 359–372, [arXiv:0912.2104](#) [hep-ph].
- [5] R. V. Harlander and K. J. Ozeren, *Finite top mass effects for hadronic Higgs production at next-to-next-to-leading order*, *JHEP* **11** (2009) 088, [arXiv:0909.3420](#) [hep-ph].
- [6] A. Pak, M. Rogal, and M. Steinhauser, *Finite top quark mass effects in NNLO Higgs boson production at LHC*, *JHEP* **02** (2010) 025, [arXiv:0911.4662](#) [hep-ph].
- [7] S. Marzani, R. D. Ball, V. Del Duca, S. Forte, and A. Vicini, *Higgs production via gluon-gluon fusion with finite top mass beyond next-to-leading order*, *Nucl. Phys.* **B800** (2008) 127–145, [arXiv:0801.2544](#) [hep-ph].

- [8] LHC Higgs Cross Section Working Group, D. de Florian *et al.*, *Handbook of LHC Higgs Cross Sections: 4. Deciphering the Nature of the Higgs Sector*, [arXiv:1610.07922](#) [hep-ph].
- [9] C. Anastasiou, C. Duhr, F. Dulat, E. Furlan, T. Gehrmann, F. Herzog, A. Lazopoulos, and B. Mistlberger, *High precision determination of the gluon fusion Higgs boson cross-section at the LHC*, *JHEP* **05** (2016) 058, [arXiv:1602.00695](#) [hep-ph].
- [10] K. Melnikov and A. Penin, *On the light quark mass effects in Higgs boson production in gluon fusion*, *JHEP* **05** (2016) 172, [arXiv:1602.09020](#) [hep-ph].
- [11] T. Neumann and C. Williams, *The Higgs boson at high p_T* , *Phys. Rev.* **D95** no. 1, (2017) 014004, [arXiv:1609.00367](#) [hep-ph].
- [12] J. M. Lindert, K. Kudashkin, K. Melnikov, and C. Wever, *Higgs bosons with large transverse momentum at the LHC*, *Phys. Lett.* **B782** (2018) 210–214, [arXiv:1801.08226](#) [hep-ph].
- [13] S. P. Jones, M. Kerner, and G. Luisoni, *Next-to-Leading-Order QCD Corrections to Higgs Boson Plus Jet Production with Full Top-Quark Mass Dependence*, *Phys. Rev. Lett.* **120** no. 16, (2018) 162001, [arXiv:1802.00349](#) [hep-ph].
- [14] T. Neumann, *NLO Higgs+jet production at large transverse momenta including top quark mass effects*, *J. Phys. Comm.* **2** no. 9, (2018) 095017, [arXiv:1802.02981](#) [hep-ph].
- [15] R. V. Harlander, T. Neumann, K. J. Ozeren, and M. Wiesemann, *Top-mass effects in differential Higgs production through gluon fusion at order α_s^4* , *JHEP* **08** (2012) 139, [arXiv:1206.0157](#) [hep-ph].
- [16] T. Neumann and M. Wiesemann, *Finite top-mass effects in gluon-induced Higgs production with a jet-veto at NNLO*, *JHEP* **11** (2014) 150, [arXiv:1408.6836](#) [hep-ph].
- [17] F. Caola, J. M. Lindert, K. Melnikov, P. F. Monni, L. Tancredi, and C. Wever, *Bottom-quark effects in Higgs production at intermediate transverse momentum*, *JHEP* **09** (2018) 035, [arXiv:1804.07632](#) [hep-ph].
- [18] J. M. Lindert, K. Melnikov, L. Tancredi, and C. Wever, *Top-bottom interference effects in Higgs plus jet production at the LHC*, *Phys. Rev. Lett.* **118** no. 25, (2017) 252002, [arXiv:1703.03886](#) [hep-ph].

- [19] R. Harlander and P. Kant, *Higgs production and decay: Analytic results at next-to-leading order QCD*, *JHEP* **12** (2005) 015, [arXiv:hep-ph/0509189](#) [hep-ph].
- [20] C. Anastasiou, S. Beerli, S. Bucherer, A. Daleo, and Z. Kunszt, *Two-loop amplitudes and master integrals for the production of a Higgs boson via a massive quark and a scalar-quark loop*, *JHEP* **01** (2007) 082, [arXiv:hep-ph/0611236](#) [hep-ph].
- [21] U. Aglietti, R. Bonciani, G. Degrossi, and A. Vicini, *Analytic Results for Virtual QCD Corrections to Higgs Production and Decay*, *JHEP* **01** (2007) 021, [arXiv:hep-ph/0611266](#) [hep-ph].
- [22] J. Fleischer, O. V. Tarasov, and V. O. Tarasov, *Analytical result for the two loop QCD correction to the decay $H \rightarrow 2\gamma$* , *Phys. Lett.* **B584** (2004) 294–297, [arXiv:hep-ph/0401090](#) [hep-ph].
- [23] M. Steinhauser, *Corrections of $O(\alpha_s^2)$ to the decay of an intermediate mass Higgs boson into two photons*, in *The Higgs puzzle – what can we learn from LEP-2, LHC, NLC and FMC? Proceedings, Ringberg Workshop, Tegernsee, Germany, December 8-13, 1996*, pp. 177–185. 1996. [arXiv:hep-ph/9612395](#) [hep-ph].
- [24] P. Maierhöfer and P. Marquard, *Complete three-loop QCD corrections to the decay $H \rightarrow \gamma\gamma$* , *Phys. Lett.* **B721** (2013) 131–135, [arXiv:1212.6233](#) [hep-ph].
- [25] R. V. Harlander and K. J. Ozeren, *Top mass effects in Higgs production at next-to-next-to-leading order QCD: Virtual corrections*, *Phys. Lett.* **B679** (2009) 467–472, [arXiv:0907.2997](#) [hep-ph].
- [26] A. Pak, M. Rogal, and M. Steinhauser, *Virtual three-loop corrections to Higgs boson production in gluon fusion for finite top quark mass*, *Phys. Lett.* **B679** (2009) 473–477, [arXiv:0907.2998](#) [hep-ph].
- [27] R. Gröber, A. Maier, and T. Rauh, *Reconstruction of top-quark mass effects in Higgs pair production and other gluon-fusion processes*, *JHEP* **03** (2018) 020, [arXiv:1709.07799](#) [hep-ph].
- [28] J. Davies, R. Gröber, A. Maier, T. Rauh, and M. Steinhauser, *Top quark mass dependence of the Higgs-gluon form factor at three loops*, [arXiv:1906.00982](#) [hep-ph].
- [29] P. Nogueira, *Automatic Feynman Graph Generation*, *J.Comput.Phys.* **105** (1993) 279–289.

- [30] R. Harlander, T. Seidensticker, and M. Steinhauser, *Corrections of $\mathcal{O}(\alpha\alpha_s)$ to the decay of the Z boson into bottom quarks*, *Phys.Lett.* **B426** (1998) 125–132, [arXiv:hep-ph/9712228](#) [hep-ph].
- [31] T. Seidensticker, *Automatic application of successive asymptotic expansions of Feynman diagrams*, [arXiv:hep-ph/9905298](#) [hep-ph].
- [32] J. A. M. Vermaseren, *New features of FORM*, [arXiv:math-ph/0010025](#) [math-ph].
- [33] T. van Ritbergen, A. Schellekens, and J. Vermaseren, *Group theory factors for Feynman diagrams*, *Int.J.Mod.Phys.* **A14** (1999) 41–96, [arXiv:hep-ph/9802376](#) [hep-ph].
- [34] F. V. Tkachov, *A theorem on analytical calculability of 4-loop renormalization group functions*, *Phys. Lett.* **100B** (1981) 65–68.
- [35] K. G. Chetyrkin and F. V. Tkachov, *Integration by parts: The algorithm to calculate β -functions in 4 loops*, *Nucl. Phys.* **B192** (1981) 159–204.
- [36] S. Laporta, *High-precision calculation of multiloop Feynman integrals by difference equations*, *Int. J. Mod. Phys.* **A15** (2000) 5087–5159, [arXiv:hep-ph/0102033](#) [hep-ph].
- [37] P. Maierhöfer, J. Usovitsch, and P. Uwer, *Kira—A Feynman integral reduction program*, *Comput. Phys. Commun.* **230** (2018) 99–112, [arXiv:1705.05610](#) [hep-ph].
- [38] P. Maierhöfer and J. Usovitsch, *Kira 1.2 Release Notes*, [arXiv:1812.01491](#) [hep-ph].
- [39] A. V. Kotikov, *Differential equations method. New technique for massive Feynman diagram calculation*, *Phys. Lett.* **B254** (1991) 158–164.
- [40] A. V. Kotikov, *Differential equations method: the Calculation of vertex-type Feynman diagrams*, *Phys. Lett.* **B259** (1991) 314–322.
- [41] A. V. Kotikov, *Differential equation method. The calculation of N-point Feynman diagrams*, *Phys. Lett.* **B267** (1991) 123–127. [Erratum: *Phys. Lett.* **B295** (1992) 409].
- [42] T. Gehrmann and E. Remiddi, *Differential equations for two loop four point functions*, *Nucl. Phys.* **B580** (2000) 485–518, [arXiv:hep-ph/9912329](#) [hep-ph].

- [43] J. M. Henn, *Multiloop integrals in dimensional regularization made simple*, *Phys. Rev. Lett.* **110** (2013) 251601, [arXiv:1304.1806 \[hep-th\]](#).
- [44] R. N. Lee, *Reducing differential equations for multiloop master integrals*, *JHEP* **04** (2015) 108, [arXiv:1411.0911 \[hep-ph\]](#).
- [45] M. Prausa, *epsilon: A tool to find a canonical basis of master integrals*, *Comput. Phys. Commun.* **219** (2017) 361–376, [arXiv:1701.00725 \[hep-ph\]](#).
- [46] S. G. Gorishnii, *Construction of operator expansions and effective theories in the \overline{MS} scheme*, *Nucl. Phys.* **B319** (1989) 633–666.
- [47] V. A. Smirnov, *Asymptotic expansions in limits of large momenta and masses*, *Commun. Math. Phys.* **134** (1990) 109–137.
- [48] V. A. Smirnov, *Asymptotic Expansions in Momenta and Masses and Calculation of Feynman Diagrams*, *Mod. Phys. Lett.* **A10** (1995) 1485–1500, [arXiv:hep-th/9412063 \[hep-th\]](#).
- [49] V. A. Smirnov, *Applied Asymptotic Expansions in Momenta and Masses*, *Springer Tracts Mod. Phys.* **177** (2002) 1–262.
- [50] A. V. Smirnov, *FIESTA4: Optimized Feynman integral calculations with GPU support*, *Comput. Phys. Commun.* **204** (2016) 189–199, [arXiv:1511.03614 \[hep-ph\]](#).
- [51] S. Catani, *The Singular behavior of QCD amplitudes at two loop order*, *Phys. Lett.* **B427** (1998) 161–171, [arXiv:hep-ph/9802439 \[hep-ph\]](#).
- [52] D. de Florian and J. Mazzitelli, *A next-to-next-to-leading order calculation of soft-virtual cross sections*, *JHEP* **12** (2012) 088, [arXiv:1209.0673 \[hep-ph\]](#).
- [53] D. Binosi, J. Collins, C. Kaufhold, and L. Theussl, *JaxoDraw: A Graphical user interface for drawing Feynman diagrams. Version 2.0 release notes*, *Comput. Phys. Commun.* **180** (2009) 1709–1715, [arXiv:0811.4113 \[hep-ph\]](#).
- [54] J. A. M. Vermaseren, *Axodraw*, *Comput. Phys. Commun.* **83** (1994) 45–58.
- [55] E. Remiddi and J. A. M. Vermaseren, *Harmonic Polylogarithms*, *Int. J. Mod. Phys.* **A15** (2000) 725–754, [arXiv:hep-ph/9905237 \[hep-ph\]](#).
- [56] D. Maître, *HPL, a Mathematica implementation of the harmonic polylogarithms*, *Comput. Phys. Commun.* **174** (2006) 222–240, [arXiv:hep-ph/0507152 \[hep-ph\]](#).